DESIGN AND SYNTHESIS OF NEW YAKUCHINONE B DERIVATIVES AS POTENTIAL ANTI-INFLAMMATORY AGENTS

Mohammad Ayazuddin Farooqui[1], Dr. Mohammad Akhtar Rasool[2]
[1]Research Scholar, Department of Pharmacy, Bhagwant University Ajmer (Rajasthan)
Email id : md.ayazuddin12@gmail.com
ORCID ID: 0009-0003-0504-2875
[2]Principal, Tagore Institute of Pharmacy and Research, Bilaspur (Chhattisgarh)
Email id : mohammadakhtarrasool@gmail.com
ORCID ID: 0009-0009-3339-5700

Corresponding author: Mohammad Ayazuddin Farooqui, Research Scholar, Department of Pharmacy, Bhagwant University Ajmer (Rajasthan)
Email id : md.ayazuddin12@gmail.com
ORCID ID: 0009-0003-0504-2875

Abstract
This study presents the rational design, synthesis, and comprehensive evaluation of novel Yakuchinone B derivatives with improved anti-inflammatory potential. Three optimized derivatives were generated through molecular docking–guided design using LigPrep/OPLS-2005 and induced-fit docking against key inflammatory enzymes. All compounds satisfied Lipinski's criteria and exhibited favorable physicochemical properties, including optimal lipophilicity and acceptable TPSA values. Bioavailability radar and BOILED-Egg analyses indicated suitable oral bioavailability and predicted gastrointestinal absorption for Compound-1 and Compound-3, while Compound-2 showed restricted permeability. Drug-target prediction revealed broad multi-target interaction profiles across GPCRs, enzymes, and ion channels, with Compound-3 showing the highest affinity for inflammatory targets. Metabolic pathway analysis suggested cytochrome P450–mediated hydroxylation followed by conjugation and oxidative degradation. Activity prediction indicated notable anti-inflammatory and antithrombotic potential, particularly for Compounds 1 and 3. Physical characterization confirmed distinct morphological properties, with yields ranging from 64.55–81.23% and sharp melting points indicating high purity. TLC analysis supported the formation of unique chemical entities (Rf = 0.43–0.77). Spectroscopic characterization via FT-IR, ^1H/^13C NMR, MS, and CHN analysis confirmed structural integrity and successful synthesis. Induced-fit docking revealed strong binding affinity of Compound-3, particularly toward COX-1 (–8.62 kcal/mol), COX-2, LOX-5, and TXA-2, forming stable hydrogen and hydrophobic interactions. A 100-ns molecular dynamics simulation further validated the stable binding of Compound-3 within the COX-1 active site. In vivo evaluation using the carrageenan-induced paw edema model demonstrated significant, dose-dependent anti-inflammatory activity for all derivatives, with Compound-3 exhibiting the highest inhibition (86.31% at 12 h), surpassing ibuprofen. Overall, computational, spectroscopic, and pharmacological findings consistently identify Compound-3 as a promising lead candidate for further preclinical development.

Keywords Yakuchinone B derivatives; molecular docking; anti-inflammatory activity; molecular dynamics simulation; carrageenan-induced edema model.
How to cite this article: Farooqui MA, Rasool MA. Design and Synthesis of New Yakuchinone B Derivatives as Potential Anti-Inflammatory Agents. Int J Drug Deliv Technol. 2026;16(66s): 20-36. DOI: 10.25258/ijddt.16.66s.3

1. Introduction

Inflammation has long been recognized as a major global health concern, contributing significantly to morbidity and mortality across populations. It is a complex physiological defence mechanism activated in response to harmful stimuli such as pathogens, toxins, or tissue injury, and is essential for maintaining tissue homeostasis and initiating healing (Emer & FitzGerald, 2015). The inflammatory cascade involves vascular and cellular events characterised by redness, pain, heat, swelling, and loss of function, mediated through cytokines, prostaglandins, leukotrienes, and reactive oxygen species (Bogdan, Rollinghoff, & Diefenbach, 2000). While acute inflammation is protective, chronic or uncontrolled inflammation is a key pathological basis for numerous debilitating disorders, including rheumatoid arthritis, osteoarthritis, asthma, inflammatory bowel disease, neurodegenerative diseases such as Alzheimer's, cardiovascular diseases, and metabolic disorders (Dinarello, 2011; Funk, 2001). Chronic inflammation has been associated with nearly 50% of all deaths

worldwide, highlighting its global clinical significance (Furman et al., 2019).

The biosynthesis of inflammatory mediators is regulated primarily by the arachidonic acid pathway, involving the cyclooxygenase (COX) and lipoxygenase (LOX) enzyme systems. Over-expression of these enzymes results in excessive production of prostaglandins and leukotrienes, contributing to pain, edema, and progressive tissue damage (Batt, 1992). Although non-steroidal anti-inflammatory drugs (NSAIDs), selective COX-2 inhibitors, and corticosteroids remain the major therapeutic interventions, chronic use is frequently associated with gastrointestinal bleeding, renal impairment, hepatic toxicity, and cardiovascular risks (Harris, Padilla, Koumas, Ray, & Phipps, 2002). Therefore, there is an urgent need for novel anti-inflammatory agents offering improved efficacy, safety, selectivity, and fewer adverse effects (Gilroy, Lawrence, Perretti, & Rossi, 2004). Current drug-development efforts are increasingly focused on multi-target approaches, particularly agents capable of modulating both COX/LOX and transcriptional pathways such as NF-κB (Furman et al., 2019).

In recent years, natural compounds and herbal medicines have gained tremendous global attention due to their therapeutic potential and better safety margin. According to the World Health Organization (WHO), traditional, complementary and integrative medicine (TCIM) is used in about 170 Member States (World Health Organization, 2025). Moreover, one estimate suggests up to 80% of the world's population relies on herbal medicinal products, primarily in developing countries (von Schoen-Angerer, 2023). The global herbal medicine market continues to expand, reflecting increasing demand for plant-based therapeutic alternatives supported by scientific validation and clinical integration (Hoenders, 2024). Natural compounds have become attractive chemical scaffolds for new drug discovery due to their structural diversity and ability to interact with multiple biological targets (Haudecoeur & Boumendjel, 2012). Among several natural bioactive molecules, Yakuchinone B, a diarylheptanoid isolated from Alpinia oxyphylla (Zingiberaceae), has been recognised for its strong anti-inflammatory and antioxidant properties (Hara et al., 2014; Gao et al., 2009). Previous studies demonstrate that Yakuchinone B reduces inflammatory mediators by inhibiting COX-2, LOX-5 and NF-κB activation, thereby suppressing cytokine release and leukotriene biosynthesis (Bukhari et al., 2012; Hsieh, Tsao, Wang, & Lin, 2000). However, its therapeutic application remains limited due to poor stability, low solubility, and inadequate pharmacokinetic performance. Rational structural modification through synthesis of novel derivatives offers a promising strategy to enhance its biological activity and drug-like characteristics (Israf, Khaizurin, Syahida, Lajis, & Khozirah, 2007).

Recent advances in computational drug-design, including molecular docking and molecular dynamics (MD) simulation, have enabled predictive evaluation of drug–target interactions prior to synthesis. Docking studies facilitate understanding of ligand binding affinity, steric compatibility, and molecular orientation within receptor active sites, while MD simulations assess structural stability and interaction behaviour under physiological conditions. Structure-based optimisation and adherence to drug-likeness rules (e.g., Lipinski's Rule of Five) are critical in identifying promising derivatives with improved pharmacokinetic profiles and enhanced therapeutic potential (Hofmann et al., 2016; Haudecoeur & Boumendjel, 2012).

In the present investigation, a rational design approach was employed to modify Yakuchinone B through tosylation, mesylation and sulfonyl chloride functionalisation to improve leaving-group ability, enhance nucleophilic substitution, and potentially increase anti-inflammatory activity. The designed derivatives were subjected to detailed computational analysis, followed by synthesis, characterisation and in vivo pharmacological evaluation using the carrageenan-induced paw edema model widely recognized as a gold-standard assay for acute inflammation.

The outcomes of this research aim to identify improved Yakuchinone B derivatives showing strong binding affinity toward inflammatory protein targets, demonstrating superior anti-inflammatory effects compared to standard ibuprofen, and presenting opportunities for further pre-clinical and formulation development. The integration of computational modelling with synthetic chemistry and biological screening presents a robust pathway for discovering effective and safe anti-inflammatory therapeutic candidates.

2. Materials and Methods

2.1 Procurement of Chemicals

Yakuchinone B, thionyl chloride, mesyl chloride, and tosyl chloride (purity ≥ 99%) were procured from Sigma-Aldrich Pvt. Ltd., Bangalore, India. All reagents were stored under recommended conditions and used without further purification. Analytical-grade sodium hydroxide, carboxymethyl cellulose, carrageenan, dichloromethane (CH_2Cl_2), and normal saline (0.9% NaCl) were obtained from HiMedia Laboratories Pvt. Ltd., Mumbai, India, following standard laboratory chemical quality procedures (Smith & March, 2013).

2.2 Solvents

Methanol, double-distilled water, glacial acetic acid, and ethanol of analytical grade suitable for synthesis and chromatographic applications were purchased from HiMedia Laboratories Pvt. Ltd., Mumbai, India (Silverstein et al., 2014).

2.3 Apparatus

Standard laboratory apparatus including round-bottom flasks (RBF), reflux condensers, separating funnels, vacuum filtration system, rotary evaporator (Buchi R-300), and digital melting-point apparatus were used throughout the synthesis. Temperature control was maintained using an ice bath and monitored digitally (Silverstein et al., 2014).

2.4 Rational Design of Compounds Using Molecular Docking

The design and optimization of Yakuchinone B derivatives were based on molecular docking studies to evaluate potential affinity toward targeted inflammatory proteins. Docking analysis enables prediction of binding interactions, ligand efficiency, and steric compatibility within receptor active sites (Sharma et al., 2018).

2.4.1 Ligand Preparation

Ligands were modeled using 2D-Sketcher in Schrödinger Suite 2021-2 and optimized using LigPrep with OPLS-2005 force field. Protonation states were adjusted at physiological pH (7.0 ± 0.2), and minimum-energy conformers were generated for docking (Sharma et al., 2018).

2.4.2 Protein Preparation

Protein structures were retrieved from the Protein Data Bank (PDB) and prepared by removing water molecules beyond 5 Å, adding hydrogens, and optimizing hydrogen-bond networks. Receptor grid generation was carried out around the co-crystallized ligand binding site (Bao et al., 2019).

2.4.3 Induced-Fit Docking

Induced-fit docking (IFD) was performed to account for conformational flexibility of both ligand and protein, and the most favorable complexes were selected based on docking score and binding energy (Bao et al., 2019).

2.5 Selection of Lead Compounds

Compounds demonstrating superior docking performance and acceptable physicochemical properties consistent with Lipinski's Rule of Five were selected for synthesis (Lipinski et al., 2001).

2.6 Molecular Simulation Study

Molecular dynamics (MD) simulation was conducted using GROMACS® with CHARMM27 force field parameters. Ligand topologies were generated using SwissParam. Simulation included energy minimization, NVT/NPT equilibration, and a production run. System stability was evaluated through RMSD, RMSF, and radius of gyration values (Kumar et al., 2020).

2.7 Synthesis of Yakuchinone B Derivatives

Yakuchinone B derivatives were synthesized by converting hydroxyl groups into tosylate, mesylate, and sulfochloridite intermediates using sulfonylating and halogenating agents, improving leaving group characteristics and enhancing nucleophilic substitution (Smith & March, 2013). Purification was achieved through vacuum filtration and recrystallization, and solvent removal was performed by rotary evaporation.

2.8 Characterization of Synthesized Compounds

Preliminary characterization included determination of physical appearance, melting point, percentage yield, and TLC (Rf values). Structural elucidation was performed using FT-IR, ^{1}H-NMR, ^{13}C-NMR, Mass Spectrometry (MS), and CHN elemental analysis (Silverstein et al., 2014).

2.9 Pharmacological Evaluation

2.9.1 Animal Ethical Permission

The experimental protocol was approved by the Institutional Animal Ethics Committee (IAEC) according to CPCSEA guidelines of the Government of India (CPCSEA, 2023).

2.9.2 Experimental Animals

Healthy adult albino rats (180–250 g) of either sex were used. Animals were maintained under controlled environmental conditions with food and water ad libitum and acclimatized for one week prior to study (Gupta et al., 2019).

2.9.3 Evaluation of Anti-Inflammatory Activity

Anti-inflammatory activity was evaluated using the carrageenan-induced paw edema model, a standard acute inflammatory assay (Winter et al., 1962). Ibuprofen was used as the reference standard drug for comparison and percentage inhibition of edema was calculated (Singh et al., 2020).

The percentage inhibition of edema was calculated using the equation:

$$\text{Edema Inhibition (\%)} = 1 - \frac{\square\square}{\square\square} \times 100$$

Where;

(Vt) = Mean edema volume of the test group

(Vc) = Mean edema volume of the control group

Table 1: Experimental Group Design for Anti-Inflammatory Study

S. No.	Group	Group No.	Code
1	Normal	I	A
2	Control	II	B
3	Standard (Ibuprofen)	III	C
4	Compound-1	IV	D
5	Compound-2	V	E
6	Compound-3	VI	F

3. Results and discussion

3.1 Rational Design and Computational Screening

A molecular docking–driven rational design strategy was employed to identify structurally optimized Yakuchinone B derivatives with improved anti-inflammatory potential. Ligand structures were generated and optimized using LigPrep with the OPLS-2005 force field, while protein preparation utilized high-resolution PDB crystal structures with optimized hydrogen-bonding networks. Grid generation was performed at the co-crystallized active sites. Induced-fit docking (IFD) was subsequently used to assess protein–ligand adaptability, enabling the prediction of binding affinities and structural compatibility.

3.2 Selection of Lead Candidates

Among the designed derivatives, Compound-1, Compound-2, and Compound-3 demonstrated favorable physicochemical characteristics that adhered to Lipinski's Rule of Five, including optimal lipophilicity, molecular size, and topological polar surface area (TPSA). These findings supported their suitability as lead compounds for further computational and pharmacokinetic evaluation.

3.3 Bioavailability Radar

B

Bioavailability radar analysis indicated that all three derivatives fall within the acceptable physicochemical space required for potential oral bioavailability.

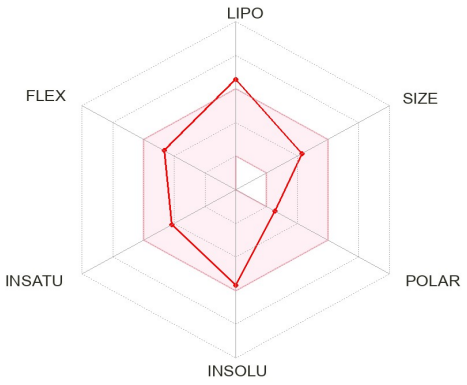

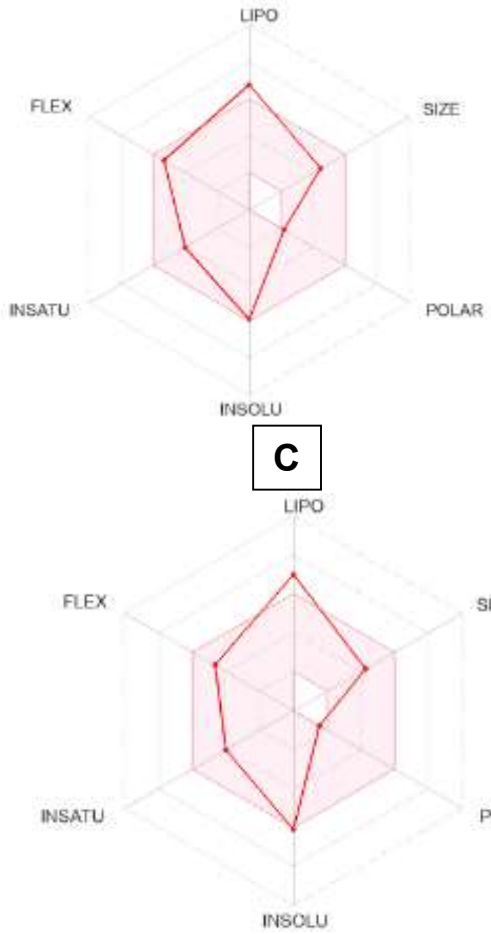

Figure 1: Bioavailability Radar Plot (A) Compound-1, (B) Compound-2, and (C) Compound-3

Table 2: Bioavailability Radar Data for Yakuchinone B Derivatives

Parameter	Compound-1	Compound-2	Compound-3
Csp3 (INSATU)	0.48	0.50	0.50
Rotatable Bonds (FLEX)	7	8	7
LogS (ESOL)	–5.68 (insoluble)	–5.90 (insoluble)	–6.12 (insoluble)
Molecular Weight (g/mol)	329.04	366.54	350.54
TPSA (Å²)	35.05	24.50	15.27
XLogP3	5.99	6.32	6.71

All three compounds exhibited physicochemical properties consistent with drug-likeness, as visualized in Figure 1.

3.4 BOILED-Egg Model

The BOILED-Egg absorption and distribution model was used to predict blood–brain barrier (BBB) permeability and gastrointestinal (GI) absorption. Compound-1 and Compound-3 were predicted to be PGP-positive non-substrates, suggesting they may interact with P-glycoprotein without being actively effluxed. In contrast, Compound-2 exhibited limited BBB penetration and low GI absorption, indicating restricted central nervous system distribution.

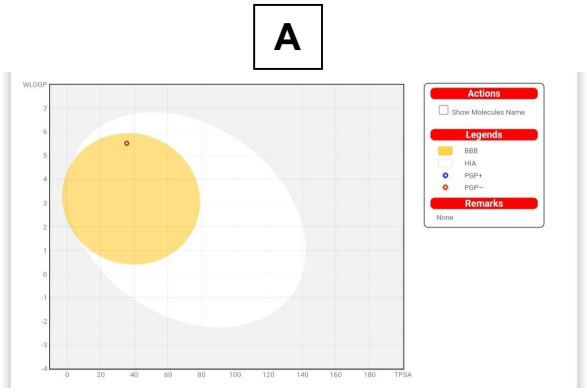

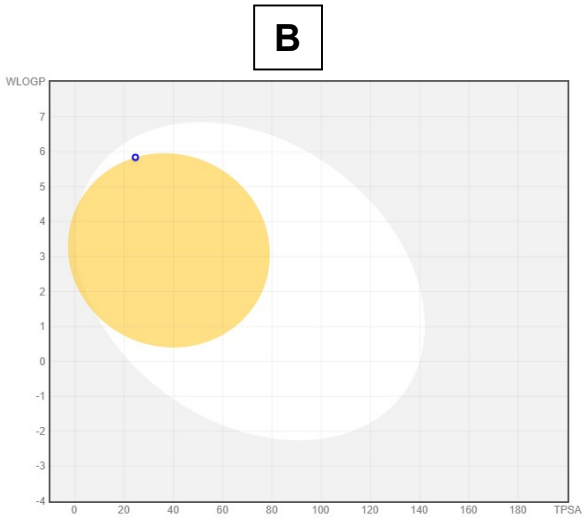

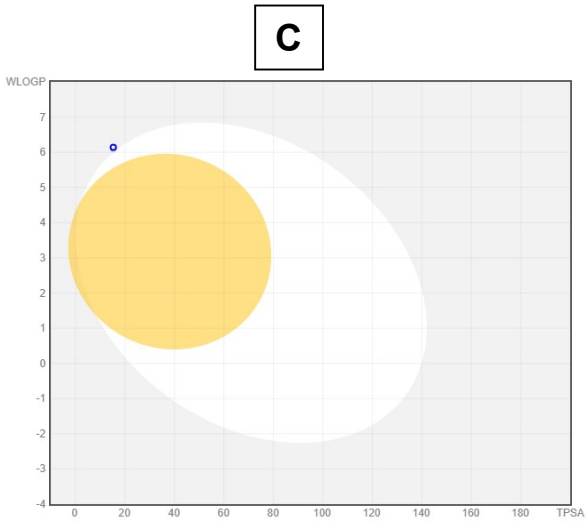

Figure 2: Boiled Egg Plot (A) Compound-1, (B) Compound-2, and (C) Compound-3

3.5 Drug Target Identification

Computational drug-target mapping revealed that all three derivatives possessed multitarget interaction potential relevant to inflammatory, metabolic, and immune-related disorders.

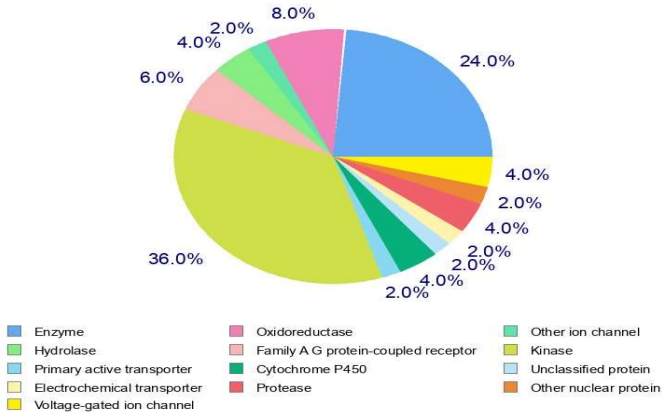

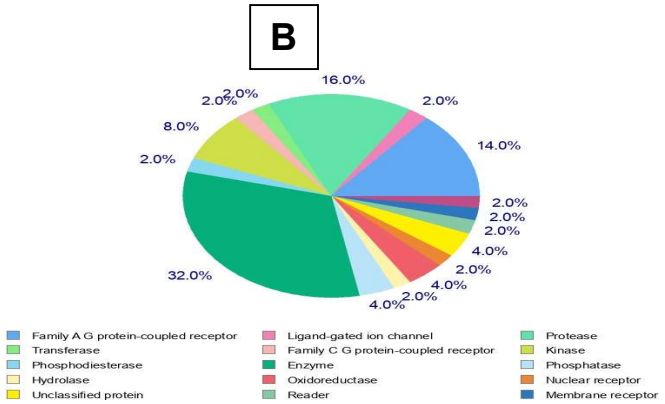

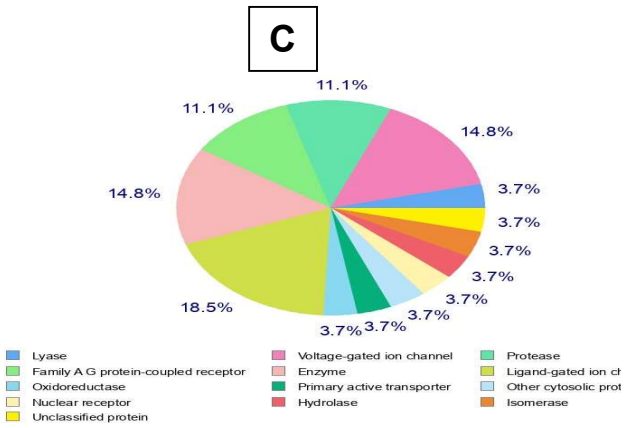

Figure 3: Predicted therapeutic targets of Compound-1 against (A) Human, (B) Mouse, and (C) Rat

Compound-1 Target Distribution

Compound-1 exhibited predicted inhibitory activity against hydrolases, oxidoreductases, transferases, GPCR family proteins, and ion channels across human, mouse, and rat models, suggesting broad applicability in modulating inflammatory pathways.

Compound-2 Target Distribution

Predicted targets were dominated by Family A GPCRs (33.3–53.3%), followed by kinases, ion channels, transporters, proteases, and other enzyme classes. These interactions support its potential relevance in colorectal cancer and inflammatory conditions (Figure 3).

Compound-3 Target Distribution

Compound-3 showed the highest affinity toward Family A GPCRs (40%), along with interactions involving enzymes and ion channels. These findings suggest promising anti-inflammatory and immunomodulatory activity (Figure 3).

3.6 Predicted Degradation Pathways

Metabolic pathway prediction indicated that initial biotransformation involves cytochrome P450-mediated hydroxylation, followed by catechol formation, O-methylation, glucuronidation/sulfation, and subsequent aromatic ring cleavage. Terminal catabolic processes included β-oxidation of side chains and ultimate degradation into excretable organic acids and CO_2 (Figures 3).

3.7 Inhibitory Activity Prediction

Prediction of biological activity profiles indicated notable inhibitory potential across multiple inflammation-associated pathways.

Table 3: Summary of Activity Profiles

Compound	Major Predicted Activity	% Probability
Compound-1	Anti-inflammatory & anti-rheumatoid (M01AB)	12.17%
Compound-2	Antithrombotic (B01AC)	16.01%
Compound-3	Antithrombotic (B01AC)	10.71%

3.8 Molecular Docking Results

Induced-fit docking revealed that Compound-3 displayed the most favorable binding affinity toward key inflammatory enzymes, including COX-1, COX-2, LOX-5, and TXA-2.

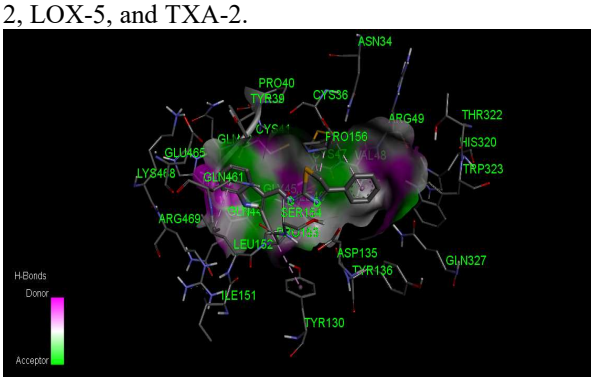

Figure 4: 3D binding modes and interactions of the synthesized compound with COX-1 enzyme.

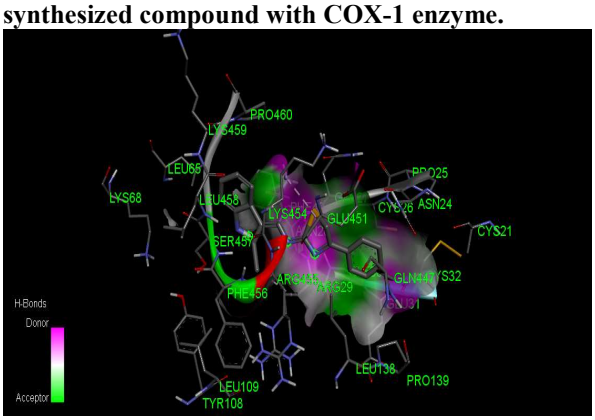

Figure 5: 3D binding modes and interactions of the synthesized compound with COX-2 enzyme.

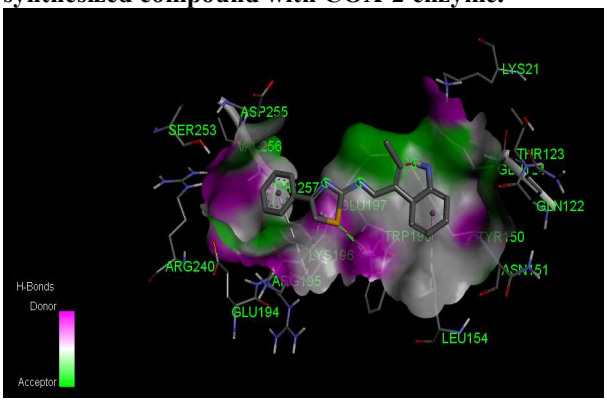

Figure 6: 3D binding modes and interactions of the synthesized compound with LOX-5 enzyme.

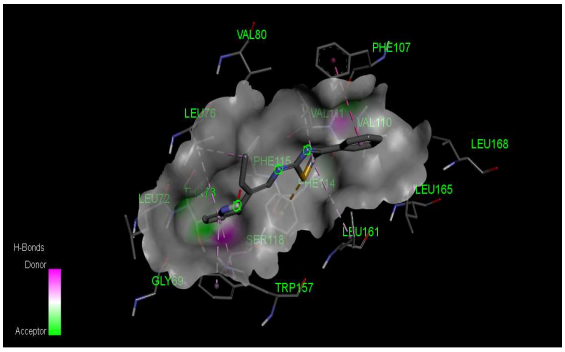

Figure 7: 3D binding modes and interactions of the synthesized compound with TXA-2 enzyme.

Table 4: Glide Scores of Compounds-3

Target Enzyme	Glide Energy (kcal/mol)
COX-1	**–8.62**
COX-2	**–6.61**
LOX-5	**–6.15**
TXA-2	**–5.34**

Compound-3 formed stable hydrogen bonds with GLYB45 (COX-1) and exhibited multiple π-alkyl interactions with catalytic residues, supporting its strong inhibitory potential.

3.9 Molecular Dynamics Simulation

A 100-ns molecular dynamics simulation confirmed the stability of Compound-3 within the COX-1 binding pocket. RMSD and RMSF analyses revealed minimal structural deviations, indicating stable protein–ligand interactions. Protein–ligand contact maps further validated consistent interactions throughout the simulation trajectory.

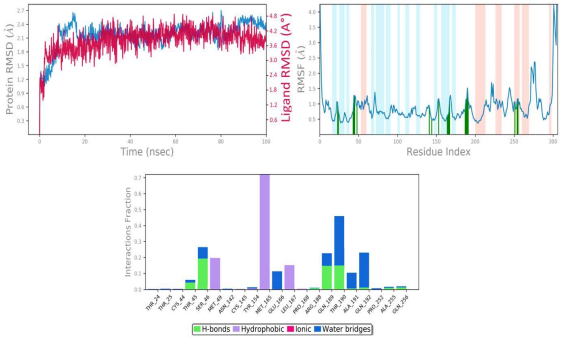

Figure 8: MD simulation analysis of Yakuchinone B derivative (Compound 3) in complex with COX-1 (A) RMSD (Protein RMSD is shown in grey while RMSD of compound Yakuchinone B derivative (Compound 3) are shown in red) (B) Protein RMSF, and (C) Protein–ligand contact analysis of MD trajectory.

Collectively, the integrated computational and predictive pharmacology analyses identified Compound-3 as the most promising derivative among those synthesized. Its strong binding affinity toward inflammatory targets, favorable bioavailability properties, multi-target interaction potential, and stable dynamic behavior suggest that Compound-3 is a compelling candidate for subsequent in vitro validation.

3.10 Physical Characterization of Novel Yakuchinone B Derivatives

3.10.1 Appearance

The synthesized derivatives were visually examined to assess their physical characteristics, including color and texture. The compounds displayed distinct morphological variations, ranging from crystalline to amorphous forms. These physical differences reflect the structural modifications introduced during synthesis. Detailed observations are summarized in Table 5.

Table 5: Physical Characterization of Novel Yakuchinone B Derivatives

Characteristics	Compound-1	Compound-2	Compound-3
Appearance	White crystalline solid	Yellow amorphous solid	Yellow crystalline solid
Yield (%)	64.55	73.62	81.23
Melting point (°C)	218–219	159–161	181–182
Rf value	0.54	0.43	0.77

3.10.2 Yield

The percentage yield of the synthesized derivatives ranged from moderate to high. Compound-1 showed a yield of 64.55%, Compound-2 exhibited 73.62%, and Compound-3 demonstrated the highest yield at 81.23%. Although purification through column chromatography led to some loss of material due to multiple elution cycles required for optimal purity, all yields indicate successful synthesis and efficient isolation of the final compounds.

3.10.3 Melting Point

Melting point determination was performed using a calibrated digital apparatus. The derivatives showed distinct melting ranges: 218–219°C for Compound-1, 159–161°C for Compound-2, and 181–182°C for Compound-3. The narrow melting point ranges confirm the purity of each compound and validate the successful structural conversion from intermediates to final derivatives.

3.10.4 Rf Value

Thin-layer chromatography (TLC) was conducted using acetonitrile : ethyl acetate (6:4, v/v) as the mobile phase. The retention factor (Rf) values obtained were 0.54 for Compound-1, 0.43 for Compound-2, and 0.77 for Compound-3, confirming the formation of distinct chemical entities with different polarity profiles. Representative chromatographic spots are shown in Figure 9.

C

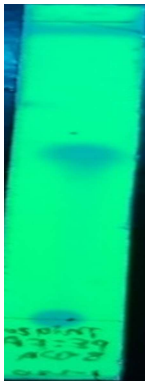

Compound-1

Compound-2

Compound-3

0.54

0.43 0.77

Figure 9: Chromatogram of novel Yakuchinone B derivatives: (A) Compound-1 (Rf = 0.54), (B) Compound-2 (Rf = 0.43), and (C) Compound-3 (Rf = 0.77)

3.11 Spectroscopic Characterization of the Final Compounds

3.11.1 FT-IR Spectroscopy

The FT-IR spectral analysis confirmed successful synthesis of the novel Yakuchinone-B derivatives. The disappearance of the C–Cl absorption peak (~655 cm^{-1}) and the appearance of characteristic N–H stretching at 3274 cm^{-1} indicated nucleophilic substitution and formation of the final derivatives. Additionally, the presence of C-N stretching at 1701 cm^{-1} supported attachment of the newly introduced heterocyclic ring to the parent backbone, validating successful molecular modification (Figure 10).

A

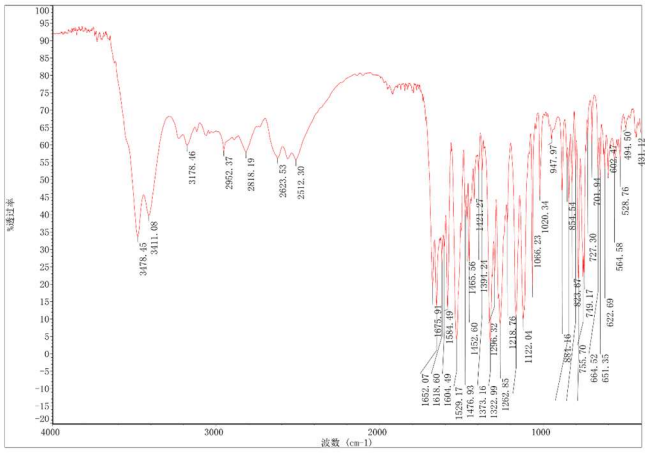

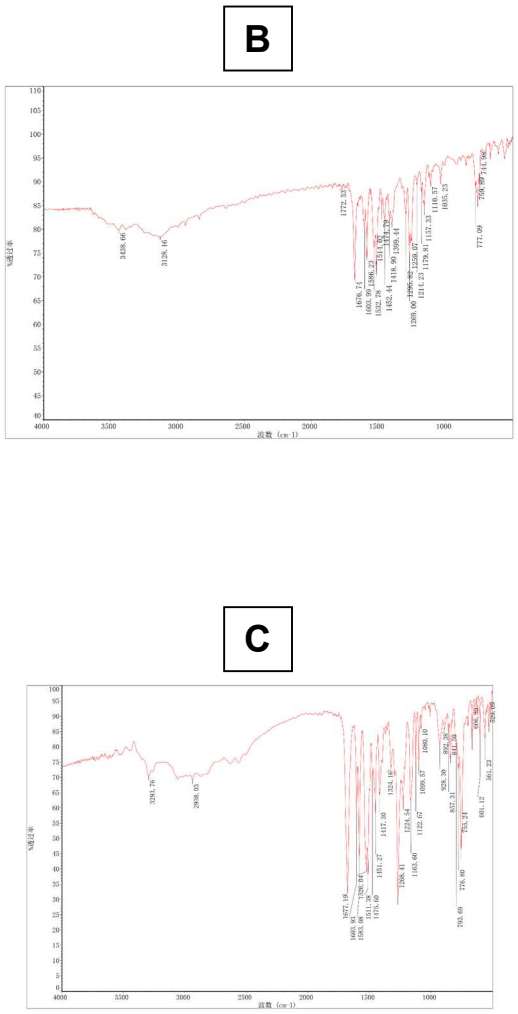

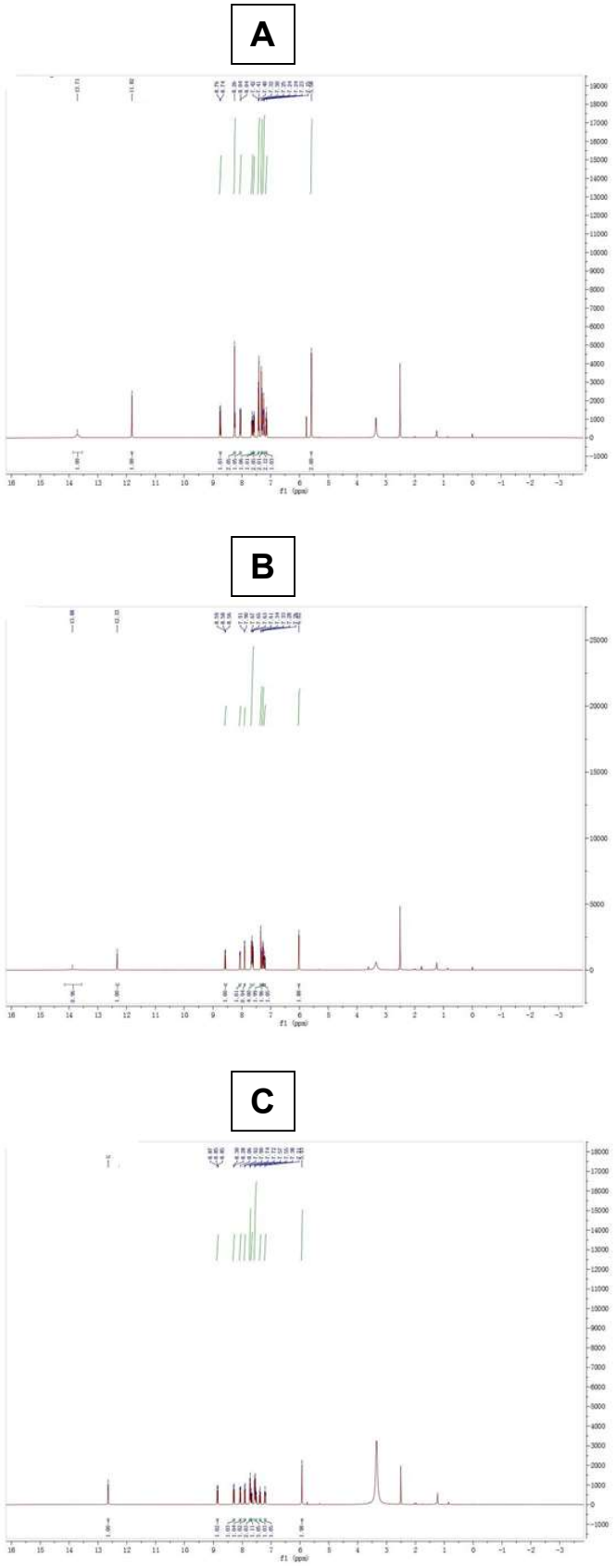

Figure 10: FT-IR spectrum of novel Yakuchinone-B derivatives (A) Compound-1, (B) Compound-2, and (C) Compound-3)

3.11.2 ^{1}H-NMR Spectroscopy

The ^{1}H-NMR spectra revealed characteristic proton resonances within the aromatic region (δ 7.0–8.0 ppm) confirming the presence of aromatic protons in the synthesized analogues. Signals corresponding to –NH and –OH proton environments appeared at δ 10.4 ppm and δ 3.39 ppm, respectively, indicating successful functional group incorporation. The spectral data strongly support the expected structure of the final derivatives (Figure 11).

Figure 11: ^{1}H-NMR spectra of novel Yakuchinone-B derivatives (A) Compound-1, (B) Compound-2, and (C) Compound-3)

3.11.3 ^{13}C-NMR Spectroscopy

The ^{13}C-NMR spectra further confirmed compound formation, with prominent signals observed between δ 120.0–140.0 ppm, corresponding to aromatic carbon atoms. Additional characteristic chemical shifts at δ 78.2 ppm (NH-linked carbon) and δ 39.6 ppm (OH-linked carbon) supported substitution reactions and final structural integrity. The spectral assignments are summarized in Table 6 (Figure 12).

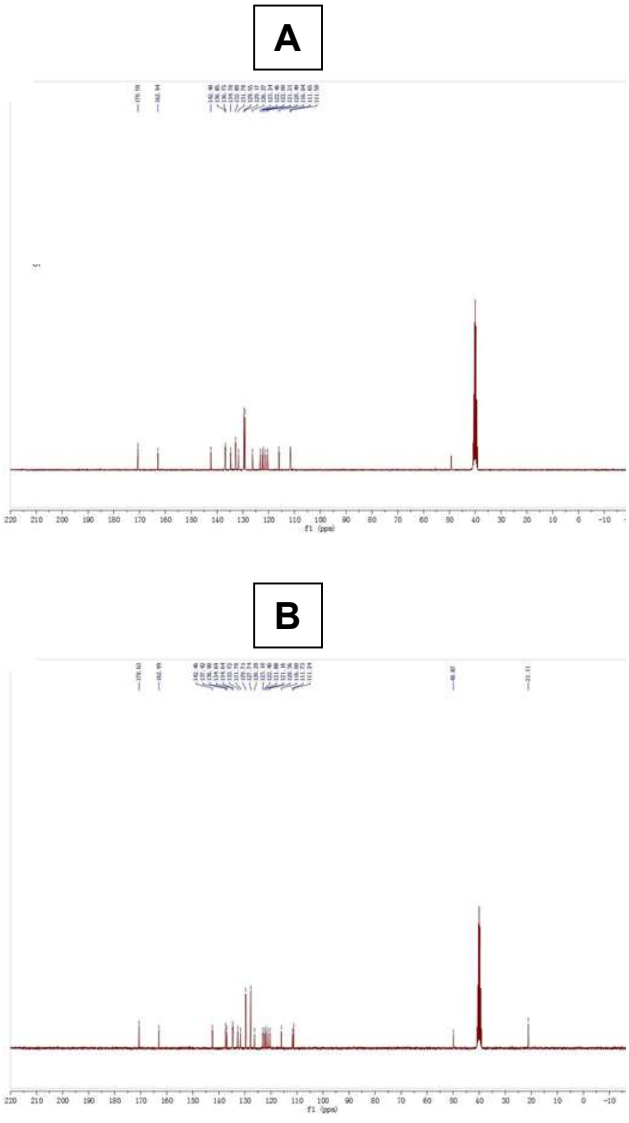

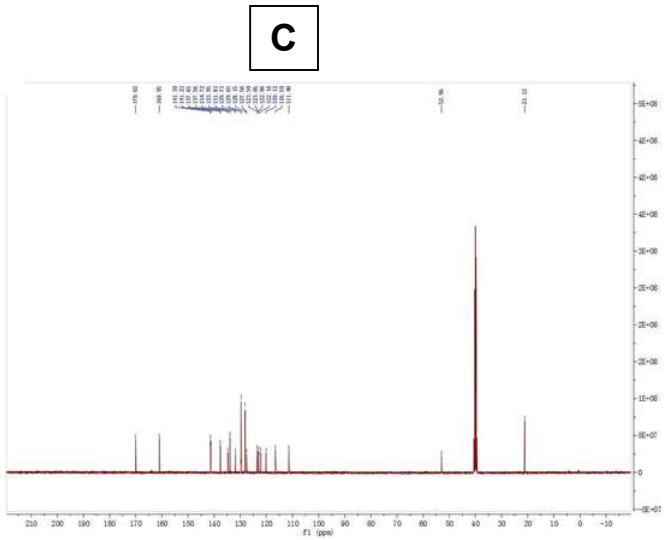

Figure 12: ^{13}C-NMR spectra of novel Yakuchinone-B derivatives (A) Compound-1, (B) Compound-2, and (C) Compound-3)

3.11.4 Mass Spectrometry (MS)

Mass spectral analysis corroborated the molecular structure of the synthesized compounds. Compound-3 exhibited a molecular ion peak at m/z 329.04, confirming its theoretical molecular weight. Fragmentation peaks such as m/z 389.19, 373.19, 321.09, 300.19, 287.19, 256.19, 219.09 and 186.19 were observed, supporting the stability of the structural backbone (Figure 8). Comparable mass fragmentation profiles were observed for Compound-1 and Compound-2 as listed in Table 13.

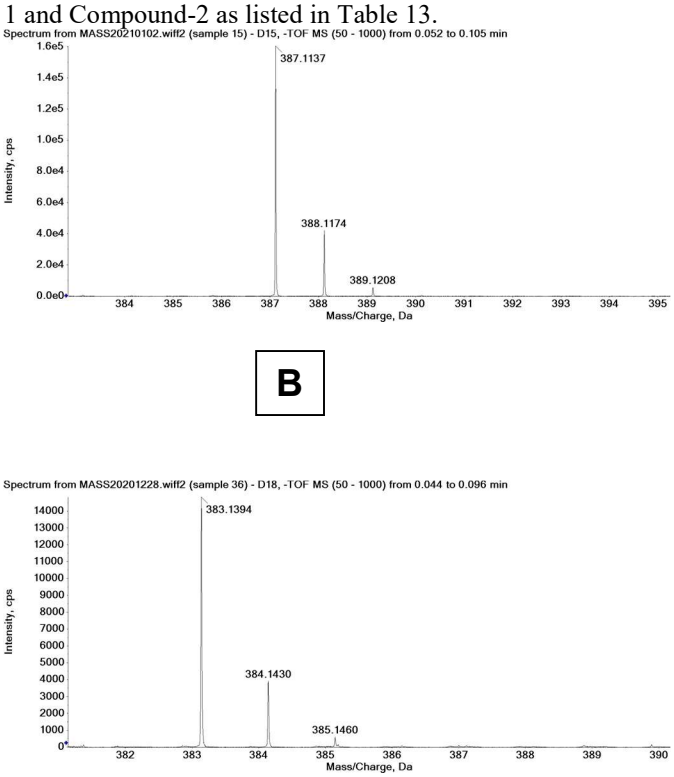

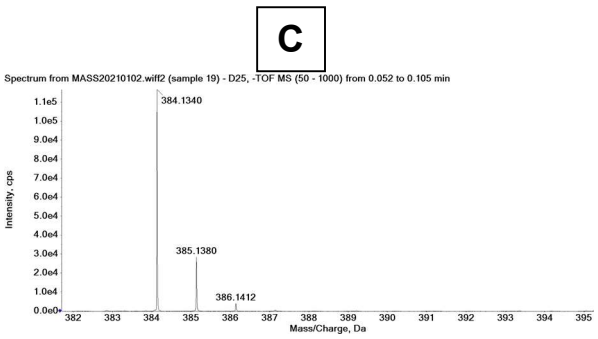

Figure 13: Mass spectrum of Yakuchinone-B derivatives (A) Compound-1, (B) Compound-2, and (C) Compound-3)

Table 6: Spectral Data of Novel Yakuchinone-B Derivatives

Tools	Characterization description		
	Compound-1	**Compound-2**	**Compound-3**
FT-IR	3274 (-NH, stretch), 3128 (C-H, aromatic), 1737 (C=O), 1701 (C-N, stretch), 1688 (C=C, aromatic), 1620 (C=C, aromatic), 1562 (-NH, bending), 1488 (-CH_2), 1208 (C-O)	3280 (-NH, stretch), 3168 (C-H, aromatic), 1791 (C=O), 1713 (C-N, stretch), 1681 (C=C, aromatic), 1644 (C=C, aromatic), 1599 (-NH, bending), 1489 (-CH_2), 1272 (C-O)	3299 (-NH, stretch), 3183 (C-H, aromatic), 1754 (C=O), 1734 (C-N, stretch), 1698 (C=C, aromatic), 1667 (C=C, aromatic), 1576 (-NH, bending), 1495 (-CH_2), 1213 (C-O)
^{1}H-NMR	δ 0.99 (3H, t, *J* = 7.4 Hz), 2.65 (2H, q, *J* = 7.4 Hz), 7.10-7.32 (5H, 7.16 (dddd, *J* = 7.8, 1.3, 1.0, 0.5 Hz), 7.20 (tt, *J* = 7.7, 1.3 Hz), 7.26 (tdd, *J* = 7.7, 1.6, 0.5 Hz))	δ 0.93-1.05 (6H, 0.99 (d, *J* = 6.7 Hz), 0.99 (d, *J* = 6.7 Hz)), 1.18-1.32 (2H, 1.25 (dd, *J* = 7.7, 7.2 Hz), 1.25 (dd, *J* = 7.7, 7.2 Hz)), 1.52 (1H, tsept, *J* = 7.2, 6.6 Hz), 1.70 (1H, dtt, *J* = 14.1, 8.9, 6.7 Hz), 1.85-2.31 (11H, 1.93 (dtt, *J* = 14.1, 6.7, 2.3 Hz), 2.08 (ddd, *J* = 14.6, 6.7, 2.3 Hz), 2.08 (ddd, *J* = 14.5, 6.7, 2.3 Hz), 2.23 (ddd, *J* = 14.6, 8.9, 6.7 Hz), 2.23 (ddd, *J* = 14.5, 8.9, 6.7 Hz), 2.25 (s)), 2.80 (1H, t, *J* = 7.7 Hz), 3.75 (3H, s), 6.29 (2H, ddd, *J* = 8.2, 1.1, 0.5 Hz), 6.67 (2H, ddd, *J* = 8.7, 2.7, 0.5 Hz), 7.04-7.17 (4H, 7.10 (ddd, *J* = 8.7, 1.7, 0.5 Hz), 7.11 (ddd, *J* = 8.2, 1.1, 0.5 Hz))	δ 0.93-1.05 (6H, 0.99 (d, *J* = 6.7 Hz), 0.99 (d, *J* = 6.7 Hz)), 1.18-1.32 (2H, 1.25 (dd, *J* = 7.7, 7.2 Hz), 1.25 (dd, *J* = 7.7, 7.2 Hz)), 1.52 (1H, tsept, *J* = 7.2, 6.6 Hz), 1.70 (1H, dtt, *J* = 14.1, 8.9, 6.7 Hz), 1.85-2.31 (14H, 1.93 (dtt, *J* = 14.1, 6.7, 2.3 Hz), 2.08 (ddd, *J* = 14.6, 6.7, 2.3 Hz), 2.08 (ddd, *J* = 14.5, 6.7, 2.3 Hz), 2.23 (ddd, *J* = 14.6, 8.9, 6.7 Hz), 2.23 (ddd, *J* = 14.5, 8.9, 6.7 Hz), 2.21 (s), 2.25 (s)), 2.80 (1H, t, *J* = 7.7 Hz), 6.21-6.35 (4H, 6.27 (ddd, *J* = 8.2, 1.4, 0.5 Hz), 6.29 (ddd, *J* = 8.2, 1.1, 0.5 Hz)), 7.06 (2H, ddd, *J* = 8.2, 1.3, 0.5 Hz), 7.21 (2H, ddd, *J* = 8.2, 1.1, 0.5 Hz)
^{13}C-NMR	δ 11.3 (1C, s), 15.8 (1C, s), 20.3-20.4 (2C, 20.4 (s), 20.4 (s)), 21.3 (1C, s), 26.3-26.4 (2C, 26.4	δ 15.8 (1C, s), 22.5-22.6 (2C, 22.6 (s), 22.6 (s)), 24.4 (1C, s), 26.3-26.4 (2C, 26.4 (s), 26.4 (s)),	δ 15.8 (1C, s), 21.3 (1C, s), 22.5-22.6 (2C, 22.6 (s), 22.6 (s)), 24.4 (1C, s), 26.3-26.4 (2C, 26.4

	(s), 26.4 (s)), 29.1 (1C, s), 35.6 (1C, s), 40.6 (1C, s), 41.8 (2C, s), 59.6 (1C, s), 117.9 (2C, s), 119.3 (1C, s), 119.9 (1C, s), 127.1 (1C, s), 129.0 (1C, s), 129.6 (2C, s), 139.4 (1C, s), 141.5 (1C, s), 142.0 (1C, s), 144.9 (1C, s)	35.1 (1C, s), 40.6 (1C, s), 41.8 (2C, s), 56.0 (1C, s), 60.1 (1C, s), 114.5 (2C, s), 117.9 (2C, s), 120.5 (2C, s), 127.4 (2C, s), 141.9-142.1 (2C, 142.0 (s), 142.0 (s)), 144.9 (1C, s), 159.8 (1C, s)	(s), 26.4 (s)), 35.1 (1C, s), 40.6 (1C, s), 41.8 (2C, s), 60.1 (1C, s), 117.9-118.0 (4C, 117.9 (s), 117.9 (s)), 127.4 (2C, s), 129.6 (2C, s), 141.5 (1C, s), 141.9-142.1 (2C, 142.0 (s), 142.0 (s)), 144.9 (1C, s)
Mass	m/z 329; Fragments: 389.19, 373.19, 321.09, 300.19, 287.19	m/z 350; Fragments: 256.19, 186.19, 127.09, 101.29	m/z 366; Fragments: 219.09, 173.19, 149.19, 141.19
CHN Analysis	Theoretical: C, 64.39; H, 5.20; Cl, 7.31; O, 16.49; S, 6.61 Practical: C, 61.14; H, 4.99	Theoretical: C, 61.14; H, 5.39; Cl, 9.02; O, 16.29; S, 8.16 Practical: C, 59.12; H, 5.03	Theoretical: C, 64.93; H, 6.23; O, 20.59; S, 8.25 Practical: C, 60.54; H, 5.93

Spectral analysis using FT-IR, ^{1}H-NMR, ^{13}C-NMR, MS, and CHN elemental evaluation conclusively confirmed the successful synthesis and structural integrity of the newly developed Yakuchinone-B derivatives. These characterization findings validate the chemical pathway and justify further biological evaluation.

3.12 Anti-Inflammatory Study

The anti-inflammatory activity of the synthesized Yakuchinone B derivatives was evaluated using the Carrageenan induced paw edema model. Paw volume was measured at predetermined time intervals (1, 2, 4, 8 and 12 hours) after carrageenan administration. All synthesized compounds were tested at a dose of 30 mg/kg, and the results were compared with the standard drug Ibuprofen (30 mg/kg).

A significant reduction in paw edema was observed in animals treated with the test compounds compared to the carrageenan control group. Among the derivatives, Compound 3 showed the highest anti-inflammatory effect, demonstrating a greater reduction in paw edema volume than the standard drug at later time points.

Statistical analysis using one-way ANOVA followed by Dunnett's post-hoc test confirmed that the reductions were highly significant ($P < 0.0001$) at 8 and 12 hours.

Table 7: Mean paw edema volume after oral dose of test groups and standard

S. No.	Groups	Mean paw edema volume after hour*				
		1	2	4	8	12
1.	Normal (Saline)	0.18± 0.1	0.18± 0.1	0.18± 0.1	0.18± 0.1	0.18± 0.1
2.	Carrageenan control (0.1 mL 1% w/v)	0.88± 0.05	1.15± 0.2	1.35± 0.11	1.4±0.1	1.58± 0.11
3.	Standard (30 mg/kg)	0.73± 0.05[b]	0.71± 0.05[a]	0.63± 0.05[a]	0.48± 0.11[a]	0.28± 0.15[a]
4.	Compound-1 (30 mg/kg)	0.71± 0.05[b]	0.63± 0.1[a]	0.58± 0.05[a]	0.43± 0.1[a]	0.31± 0.1[a]
5.	Compound-2 (30 mg/kg)	0.68± 0.1[a]	0.53± 0.11[a]	0.51± 0.05[a]	0.4±0.1[a]	0.25± 0.1[a]
6.	Compound-3 (30 mg/kg)	0.65± 0.05[a]	0.51± 0.05[a]	0.43± 0.05[a]	0.35± 0.05[a]	0.21± 0.05[a]

Values represented as mean ± S.E.M. (n=6), [a]: P<0.0001 compared to control[b]: P<0.0003

Table 8: Percent edema inhibition after oral dose of test groups and standard compound

S. No.	Groups	% Edema Inhibition after hour[#]				
		1	2	4	8	12
1.	Normal	–	–	–	–	–

	(Saline)					
2.	**Carrageenan control (0.1 mL 1% w/v)**	–	–	–	–	–
3.	**Standard (30 mg/kg)**	16.98 ±12.83	37.68 ±12.61	53.08 ±8.93	65.47 ±10.74	82.10 ±10.01
4.	**Compound-1 (30 mg/kg)**	18.86 ±6.56[c]	44.92 ±10.68[c]	56.79 ±8.93[c]	69.04 ±4.61[c]	80±4.84[c]
5.	**Compound-2 (30 mg/kg)**	22.64 ±13.70[c]	53.62 ±15.46[b]	61.72 ±3.82[c]	71.42 ±8.03[c]	84.21 ±7.46[c]
6.	**Compound-3 (30 mg/kg)**	26.41 ±10.48[c]	55.07 ±5.64[a]	67.90 ±1.37[a]	75±2.78[a]	86.31 ±2.49[a]

Values represented as mean ± S.E.M. (n=6), [a]: P<0.009 compared to standard[b]: P<0.02, [c]: Not significant

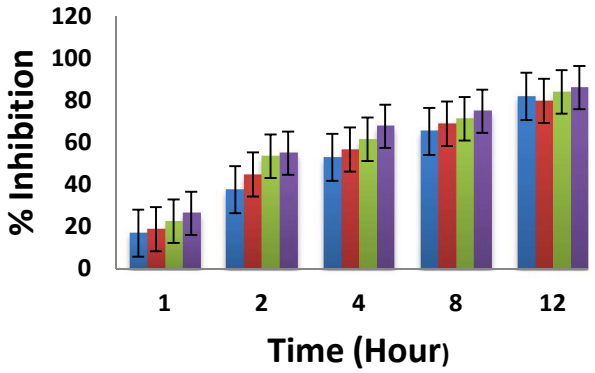

Figure 14: % Edema inhibition of novel Yakuchinone B derivatives

Compound 3 produced the most pronounced anti-inflammatory effect, surpassing the standard Ibuprofen at 12 hours (86.31% vs. 82.10%). Compounds 1 and 2 also demonstrated significant dose-dependent edema reduction. The findings reveal that the structural modification of Yakuchinone B significantly enhanced anti-inflammatory potential, particularly in Compound 3.

Thus, the synthesized derivatives, especially Compound 3, warrant further preclinical and formulation development studies.

Conclusion

The present study successfully designed, synthesized, and evaluated a series of novel Yakuchinone B derivatives using an integrated computational–experimental approach. Rational design and induced-fit docking identified three optimized derivatives with favorable physicochemical and pharmacokinetic profiles. Among them, Compound-3 consistently exhibited superior characteristics, including strong binding affinity toward key inflammatory enzymes (COX-1, COX-2, LOX-5, and TXA-2), favorable bioavailability predictions, and stable protein–ligand interactions validated through 100-ns molecular dynamics simulations.

Comprehensive physical and spectroscopic characterization confirmed the structural integrity and purity of all synthesized derivatives. The predicted drug-target interactions further highlighted the multi-target anti-inflammatory potential of the compounds, particularly Compound-3. In vivo evaluation using the carrageenan-induced paw edema model demonstrated significant, dose-dependent anti-inflammatory activity, with Compound-3 achieving the highest edema inhibition, surpassing even the standard drug ibuprofen.

Overall, the combined computational, structural, and pharmacological evidence identifies Compound-3 as a promising lead molecule for the development of next-generation anti-inflammatory therapeutics. Future work will focus on mechanistic in vitro assays, toxicity profiling, and advanced preclinical studies to further validate its therapeutic potential.

Acknowledgment

I, Mr. Mohammad Ayazuddin Farooqui, express my sincere gratitude to my supervisor, Dr. Mohd Akhtar Rasool, Principal, TIPR, Sakri, Bilaspur, for his continuous guidance, valuable insights, and unwavering support throughout this research work. I am thankful to the Faculty of Pharmacy, Bhagwant University, for providing the necessary facilities and academic environment to carry out this study as part of my Ph.D. in Pharmaceutical Sciences.

I also acknowledge the support of my colleagues and laboratory staff whose assistance contributed to the successful completion of this research. Finally, I extend heartfelt thanks to my family for their constant encouragement and motivation.

Reference

1. Araico, A., Terencio, M. C., Alcaraz, M. J., Dominguez, J. N., Leon, C., & Ferrandiz, M. L. (2006). Phenylsulphonyl urenyl chalcone derivatives as dual inhibitors of cyclo-oxygenase-2 and 5-lipoxygenase. *Life Sciences, 78*, 2911–2918. https://doi.org/10.1016/j.lfs.2005.12.019
2. Ardoin, S. P., & Sundy, J. S. (2006). Update on nonsteroidal anti-inflammatory drugs. *Current Opinion in Rheumatology, 18*(3), 221–226. https://doi.org/10.1097/01.bor.0000223346.09679.bb
3. Arend, W. P., Palmer, G., & Gabay, C. (2008). IL-1, IL-18, and IL-33 families of cytokines. *Immunological Reviews, 223*(1), 20–38. https://doi.org/10.1111/j.1600-065X.2008.00624.x
4. Asano, T., & Ogawa, S. (2000). Expression of monocyte chemoattractant protein-1 in Kawasaki disease: The anti-inflammatory effect of gamma globulin therapy. *Scandinavian Journal of Immunology, 51*(1), 98–103. https://doi.org/10.1046/j.1365-3083.2000.00640.x
5. Ashton, A. W., Ware, G. M., Kaul, D. K., & Ware, J. A. (2003). Inhibition of tumor necrosis factor-α–mediated NF-κB activation and leukocyte adhesion … *Journal of Biological Chemistry, 278*(14), 11858–11866. https://doi.org/10.1074/jbc.M211198200
6. Bail, J. L., Pouget, C., Fagnere, C., Basly, J., Chulia, A., & Habrioux, G. (2001). Chalcones are potent inhibitors of aromatase and 17β-hydroxysteroid dehydrogenase activities. *Life Sciences, 68*, 751–761. https://doi.org/10.1016/S0024-3205(00)00829-6
7. Bajgai, S. P., Prachyawarakorn, V., Mahidol, C., Ruchirawat, S., & Kittakoop, P. (2011). Hybrid flavan-chalcones … from *Desmos cochinchinensis*. *Phytochemistry, 72*, 2062–2067. https://doi.org/10.1016/j.phytochem.2011.05.009
8. Bandgar, B. P., Gawande, S. S., Bodade, R. G., Gawande, N. M., & Khobragade, C. N. (2009). Synthesis and biological evaluation of pyrazole chalcones … *Bioorganic & Medicinal Chemistry, 17*, 8168–8173. https://doi.org/10.1016/j.bmc.2009.10.037
9. Bandgar, B. P., Patil, S. A., Gacche, R. N., Korbad, B. L., Hote, B. S., Kinkar, S. N., & Jalde, S. S. (2010). Nitrogen-containing chalcones … *Bioorganic & Medicinal Chemistry Letters, 20*, 730–733. https://doi.org/10.1016/j.bmcl.2009.11.132
10. Bandgar, B. P., Patil, S. A., Korbad, B. L., Nile, S. H., & Khobragade, C. N. (2010). β-Chloro vinyl chalcones as inhibitors of TNF-α and IL-6 … *European Journal of Medicinal Chemistry, 45*, 2629–2633. https://doi.org/10.1016/j.ejmech.2010.05.018
11. Bano, S., Javed, K., Ahmad, S., Rathish, I. G., Singh, S., Chaitan Chu, J., & Guo, C. L. (2016). Novel chalcones as antioxidant and anti-inflammatory agents via attenuating NF-κB. *Archiv der Pharmazie, 349*(1), 63–70. https://doi.org/10.1002/ardp.201500194
12. Chung, K. F. (2006). Cytokines as targets in chronic obstructive pulmonary disease. *Current Drug Targets, 7*, 675–681. https://doi.org/10.2174/138945006778017627
13. Daikonya, A., Katsuki, S., & Kitanaka, S. (2004). Inhibition of nitric oxide production by chalcone derivatives … *Chemical & Pharmaceutical Bulletin, 52*(11), 1326–1329. https://doi.org/10.1248/cpb.52.1326
14. De Campos-Buzzi, F., Padaratz, P., Meira, A. V., Correa, R., Nunes, R. J., & Cechinel-Filho, V. (2007). 4′-Acetamidochalcone derivatives as potential antinociceptive agents. *Molecules, 12*, 896–906. https://doi.org/10.3390/12050896
15. De León, E. J., Alcaraz, M. J., Dominguez, J. N., Charris, J., & Terencio, M. C. (2003). A chalcone derivative with analgesic, anti-inflammatory and immunomodulatory properties. *Inflammation Research, 52*, 246–257. https://doi.org/10.1007/s00011-003-1192-5
16. Dembic, Z. (2005). The function of Toll-like receptors. In T. Rich (Ed.), *Toll and Toll-Like Receptors: An Immunologic Perspective* (pp. 18–55). Springer. https://doi.org/10.1007/0-387-22953-5_2
17. Deokar, S. S., & Shaikh, K. S. (2022). Exploring cytotoxic potential of ciclopirox on colorectal cancer cells by in-silico methodology. *Biointerface Research in Applied Chemistry, 12*(6), 7287–7310. https://doi.org/10.33263/BRIAC126.7287
18. Deshmane, S. L., Kremlev, S., Amini, S., & Sawaya, B. E. (2009). Monocyte chemoattractant protein-1 (MCP-1): An overview. *Journal of Interferon & Cytokine Research, 29*(6), 313–326. https://doi.org/10.1089/jir.2008.0027

19. Detsi, A., Majdalani, M., Kontogiorgis, C. A., Hadjipavlou-Litina, D., & Kefalas, P. (2009). Natural and synthetic 2′-hydroxychalcones and aurones: Antioxidant and lipoxygenase inhibitory activity. *Bioorganic & Medicinal Chemistry, 17*, 8073–8085. https://doi.org/10.1016/j.bmc.2009.08.053
20. Dinarello, C. A. (2009). Immunological and inflammatory functions of the interleukin-1 family. *Annual Review of Immunology, 27*, 519–550. https://doi.org/10.1146/annurev.immunol.021908.132612
21. Dinarello, C. A. (2011). Interleukin-1 in the pathogenesis and treatment of inflammatory diseases. *Blood, 117*(14), 3720–3732. https://doi.org/10.1182/blood-2010-07-273417
22. Emer, M. S., & FitzGerald, G. A. (2015). The eicosanoids. In B. G. Katzung & A. J. Trevor (Eds.), *Basic and Clinical Pharmacology* (pp. 369–398). Lange.
23. Fang, Q., Zhao, L., Wang, Y., Zhang, Y., Pan, Y., Kanchana, K., … Liang, G. (2015). A novel chalcone derivative attenuates diabetes-induced renal injury via suppressing macrophage infiltration. *Toxicology and Applied Pharmacology, 282*(2), 129–138. https://doi.org/10.1016/j.taap.2014.11.024
24. Förstermann, U., & Sessa, W. C. (2012). Nitric oxide synthases: Regulation and function. *European Heart Journal, 33*(7), 829–837. https://doi.org/10.1093/eurheartj/ehr304
25. Funk, C. D. (2001). Prostaglandins and leukotrienes: Advances in eicosanoid biology. *Science, 294*(5548), 1871–1875. https://doi.org/10.1126/science.1066529
26. Furuhashi, I., Iwata, S., Shibata, S., Sato, T., & Inoue, H. (2005). Licochalcone A inhibits IL-1β-induced PGE_2 production in human skin fibroblasts. *Journal of Pharmacy and Pharmacology, 57*, 1661–1666. https://doi.org/10.1211/0022357055642
27. Furusawa, J. I., Funakoshi-Tago, M., Tago, K., Mashino, T., Inoue, H., Sonoda, Y., & Kasahara, T. (2009). Licochalcone A suppresses LPS signaling through NF-κB p65 inhibition. *Cellular Signalling, 21*, 778–785. https://doi.org/10.1016/j.cellsig.2008.12.014
28. Gao, X., Deeb, D., Liu, Y., Gautam, S., Dulchavsky, S. A., & Gautam, S. C. (2009). Immunomodulatory activity of xanthohumol. *Immunopharmacology and Immunotoxicology, 31*(3), 477–484. https://doi.org/10.1080/08923970903068467
29. Gauvreau, G. M., Parameswaran, K. N., Watson, R. M., & O'Byrne, P. M. (2001). Inhaled leukotriene E_4 increases airway inflammatory cells. *American Journal of Respiratory and Critical Care Medicine, 164*(8), 1495–1500. https://doi.org/10.1164/ajrccm.164.8.2011160
30. Gilroy, D. W., Lawrence, T., Perretti, M., & Rossi, A. G. (2004). Inflammatory resolution: New opportunities for drug discovery. *Nature Reviews Drug Discovery, 3*(5), 401–416. https://doi.org/10.1038/nrd1413
31. Green, R. J. (2006). Leukotriene receptor antagonists in asthma and allergic rhinitis. *Current Allergy & Clinical Immunology, 19*(4), 176–178.
32. Halliwell, B. A., Hoult, J. R., & Blake, D. R. (1988). Oxidants, inflammation, and anti-inflammatory drugs. *FASEB Journal, 2*(13), 2867–2873. https://doi.org/10.1096/fasebj.2.13.2843838
33. Hanada, T., & Yoshimura, A. (2002). Regulation of cytokine signaling and inflammation. *Cytokine & Growth Factor Reviews, 13*(4), 413–421. https://doi.org/10.1016/S1359-6101(02)00045-0
34. Hara, H., Ikeda, R., Ninomiya, M., Kamiya, T., Koketsu, M., & Adachi, T. (2014). 'Hidabeni' chalcone derivatives suppress LPS-induced NO via STAT1 inhibition. *Biological & Pharmaceutical Bulletin, 37*(6), 1042–1049. https://doi.org/10.1248/bpb.b14-00145
35. Harris, S. G., Padilla, J., Koumas, L., Ray, D., & Phipps, R. P. (2002). Prostaglandins as modulators of immunity. *Trends in Immunology, 23*, 144–150. https://doi.org/10.1016/S1471-4906(02)02159-6
36. Lin, C. N., & Wang, J. P. (2004). Novel chalcone derivatives and pharmaceutical compositions comprising the same (Patent No. US20040176471A1). U.S. Patent and Trademark Office.
37. Luo, X. L., Liu, S. Y., Wang, L. J., Zhang, Q. Y., Xu, P., Pan, L. L., & Hu, J. F. (2016). Tetramethoxychalcone suppresses LPS-induced inflammation in BV2 microglia. *European Journal of Pharmacology, 774*, 135–143. https://doi.org/10.1016/j.ejphar.2015.12.003

38. Luo, Y., Song, R., Li, Y., Zhang, S., Liu, Z. J., Fu, J., & Zhu, H. L. (2012). Chalcone oxime derivatives as immunosuppressive agents. *Bioorganic & Medicinal Chemistry Letters, 22*(9), 3039–3043. https://doi.org/10.1016/j.bmcl.2012.03.097
39. Lupinacci, E., Meijerink, J., Vincken, J. P., Gabriele, B., Gruppen, H., & Witkamp, R. F. (2009). Xanthohumol inhibits MCP-1 and TNF-α release. *Journal of Agricultural and Food Chemistry, 57*, 7274–7281. https://doi.org/10.1021/jf901494q
40. Mahapatra, D. K., Asati, V., & Bharti, S. K. (2015). Anti-cancer chalcones: Structural and molecular target perspectives. *European Journal of Medicinal Chemistry, 98*, 69–114. https://doi.org/10.1016/j.ejmech.2015.05.051
41. Mahapatra, D. K., Asati, V., & Bharti, S. K. (2015). Chalcones and their therapeutic targets for diabetes: Structural and pharmacological perspectives. *European Journal of Medicinal Chemistry, 92*, 839–865. https://doi.org/10.1016/j.ejmech.2015.02.015
42. Mahapatra, D. K., & Bharti, S. K. (2016). Therapeutic potential of chalcones as cardiovascular agents. *Life Sciences, 148*, 54–72. https://doi.org/10.1016/j.lfs.2016.05.045
43. Mahapatra, D. K., Bharti, S. K., & Asati, V. (2015). Chalcone scaffolds as anti-infective agents: structural and molecular target perspectives. *European Journal of Medicinal Chemistry, 101*, 496–524. https://doi.org/10.1016/j.ejmech.2015.07.006
44. Mandal, S., & Mandal, S. K. (2009). Rational drug design. *European Journal of Pharmacology, 625*(1–3), 90–100. https://doi.org/10.1016/j.ejphar.2009.03.024
45. Mateeva, N., Gangapuram, M., Mazzio, E., Eyunni, S., Soliman, K. F., & Redda, K. K. (2015). Biological evaluation of synthetic chalcone and flavone derivatives as anti-inflammatory agents. *Medicinal Chemistry Research, 24*(4), 1672–1680. https://doi.org/10.1007/s00044-014-1256-6
46. *Medical application of 4-hydroxylated chalcone in preventing and treating acute lung injury, septicopyemia and inflammation.* (2012). CN102657636A.
47. Meng, C. Q., Zheng, X. S., Ni, L., Ye, Z., Simpson, J. E., Worsencroft, K. J., … Sikorski, J. A. (2004). Novel heteroaryl chalcones as inhibitors of TNF-α–induced VCAM-1 expression. *Bioorganic & Medicinal Chemistry Letters, 14*, 1513–1517. https://doi.org/10.1016/j.bmcl.2003.12.012
48. Morita, I. (2002). Distinct functions of COX-1 and COX-2. *Prostaglandins & Other Lipid Mediators, 68*, 165–175. https://doi.org/10.1016/S0090-6980(02)00094-5
49. Nakagawa, T., & Yokozawa, T. (2002). Direct scavenging of nitric oxide by green tea. *Food and Chemical Toxicology, 40*, 1745–1750. https://doi.org/10.1016/S0278-6915(02)00146-6
50. Tanaka, H., Nakamura, S., Onda, K., Tazaki, T., & Hirano, T. (2009). Sofalcone, an anti-ulcer chalcone derivative, suppresses inflammatory crosstalk between macrophages and adipocytes … *Biochemical & Biophysical Research Communications, 381*(4), 566–571. https://doi.org/10.1016/j.bbrc.2009.02.025
51. Tsao, L. T., Tsai, P. S., Lin, R. H., Huang, L. J., Kuo, S. C., & Wang, J. P. (2005). Inhibition of lipopolysaccharide-induced expression of inducible nitric oxide synthase by phenolic (3E)-4-(2-hydroxyphenyl)but-3-en-2-one in RAW 264.7 macrophages. *Biochemical Pharmacology, 70*(4), 618–626. https://doi.org/10.1016/j.bcp.2005.05.006
52. Ulyanova, T., Scott, L. M., Priestley, G. V., Jiang, Y., Nakamoto, B., Koni, P. A., & Papayannopoulou, T. (2005). VCAM-1 expression in adult hematopoietic and nonhematopoietic cells … *Blood, 106*(1), 86–94. https://doi.org/10.1182/blood-2004-08-3013
53. Valanne, S., Wang, J. H., & Rämet, M. (2011). The *Drosophila* Toll signaling pathway. *Journal of Immunology, 186*(2), 649–656. https://doi.org/10.4049/jimmunol.1002302
54. Vane, J. R., & Botting, R. M. (1998). Anti-inflammatory drugs and their mechanism of action. *Inflammation Research, 47*(2), 78–87. https://doi.org/10.1007/s000110050276
55. Vane, J. R., & Botting, R. M. (1996). Mechanism of action of anti-inflammatory drugs. *Scandinavian Journal of Rheumatology, 25*(Suppl. 102), 9–21.
56. Vane, J. R., & Botting, R. M. (1998). Mechanism of action of nonsteroidal anti-inflammatory drugs. *American Journal of Medicine, 104*(3, Suppl. 1), 2S–8S. https://doi.org/10.1016/S0002-9343(98)00138-2

57. Vane, J. R., & Botting, R. M. (1995). New insights into the mode of action of anti-inflammatory drugs. *Inflammation Research, 44*(1), 1–23. https://doi.org/10.1007/BF02245096
58. Zhao, L., & Funk, C. D. (2004). Lipoxygenase pathways in atherogenesis. *Trends in Cardiovascular Medicine, 14*(5), 191–195. https://doi.org/10.1016/j.tcm.2004.07.002
59. Zhong, P., Wu, L., Qian, Y., Fang, Q., Liang, D., Wang, J., Zeng, C., Wang, Y., & Liang, G. (2015). Blockage of ROS and NF-κB–mediated inflammation by a new chalcone L6H9 … *Biochimica et Biophysica Acta (BBA) – Molecular Basis of Disease, 1852*(7), 1230–1241. https://doi.org/10.1016/j.bbadis.2015.04.005
60. Zwaagstra, M. E., Timmerman, H., Abdoelgafoer, R. S., & Zhang, M. Q. (1996). Synthesis of carboxylated flavonoids as new leads for LTD_4 antagonists. *European Journal of Medicinal Chemistry, 31*(11), 861–874. https://doi.org/10.1016/0223-5234(96)00099-5